JOURNAL OF MODERN OPTICS, 2001, VOL. 48, NO. 6, 1021-1033

# Validation of left-right method for scattering by a rough surface

M. SPIVACK†, A. KEEN‡, J. OGILVY‡ and C. SILLENCE‡

†Department of Applied Mathematics and Theoretical Physics, The University of Cambridge CB3 9EW, UK

‡BAE SYSTEMS, Advanced Technology Centres—Sowerby, Filton, Bristol, BS34 7QW, UK

(*Received 12 October 2000; revision received 3 November 2000*)

**Abstract.** The method of left-right splitting is studied for the calculation of electromagnetic fields on a finite, perfectly conducting, corrugated rough surface. Surface currents are evaluated for TE and TM polarizations, both on the rough surface and on an extended surface with a rough patch, and these are compared with results from a finite element time-domain calculation. Very good agreement is obtained with one or two terms in the series. The effect of surface truncation is studied for the two polarizations, together with the reflected and transmitted components to the left and right of the rough surface patch, and the TM polarization is found to be relatively insensitive to the surface truncation.

## 1. Introduction

The calculation of wave scattering due to rough surfaces continues to present major theoretical and computational challenges (e.g. [1-6]) particularly in the presence of multiple scattering. The most flexible numerical methods, allowing a high degree of multiple scattering, are those based on integral equations, but these can be computationally intensive. This is particularly acute at low grazing angles (see e.g. [7]), where multiple scattering occurs for very slight roughness, and there is an additional problem of spurious field interaction with the edge of the computational domain. The computational expense in some cases can to some extent be overcome, and much recent effort has been devoted to this. When roughness length scales are large and forward scattering predominates, the 'parabolic integral equation method' can be applied [8, 9]. For more general problems the approach of 'left-right splitting' and related methods [10, 11] have been developed: this expresses the scattered field as an iterative series of terms of increasing orders of multiple scattering, as described below. Other iterative solutions have been studied by Macaskill and Kachoyan [12].

Independent validation is vital in order to apply such methods reliably in practice. In the regime of small surface heights, $k_\sigma \ll 1$, it is possible for example to compare with perturbation theory [13] and theoretical results for the case of periodic surfaces [14, 15]. Other small parameters can be used similarly (Kirchhoff approximation [16]; or the small slope approximation [17, 18] which is accurate over a wider range of scattering angles than both of these). For arbitrary finite

*Journal of Modern Optics* ISSN 0950-0340 print/ISSN 1362-3044 online 
http://www.tandf.co.uk/journals
DOI: 10.1080/09500340010018946

rough surfaces, however, independent validation is difficult, and such results are therefore scarce. In addition edge effects must be dealt with *ad hoc*, for example by tapering the incident field [19].

In this paper the left-right splitting method is developed and applied to a set of characterized rough perfectly conducting surfaces, and the results carefully compared with finite element time-domain (FETD) calculations. This is carried out for the 2-dimensional scalar wave problem of scattering from corrugated surfaces, for both transverse electric (TE) and transverse magnetic (TM) incident fields. The principal aims are to provide a reliable validation of the integral equation calculation, to evaluate its convergence, and to examine the influence of the surface truncation or edge effects for the two polarizations.

The essence of the method is as follows. The unknown surface field is expressed in the usual way as the solution to the Helmholtz integral equation, with the integral taken over the rough surface. This may be written formally as $A\mathsf{u} = \mathsf{f}$, where $\mathsf{u}$ is the unknown surface field and $\mathsf{f}$ is the incident field, impinging from the left, say. We therefore require $\mathsf{u} = A^{-1}\mathsf{f}$. The region of integration is split into two, to the left and right of the point of observation, which allows $A$ to be written as the sum of 'left' and 'right' components, say $(L + R)\mathsf{u} = \mathsf{f}$. Roughly speaking $L$, which includes the principal value, represents scattering from the left, and $R$ the residual scattering from the right. When this system is discretized it leads to a matrix equation, in which $L$ is the lower triangular part of $A$ (including the diagonal) and $R$ is the upper triangular part. The inverse of $A$ can formally be expressed as a series

$$A^{-1} = L^{-1} - L^{-1}RL^{-1} + \cdots .$$

Under the assumption that most energy is right-going, $L$ is the dominant part of the matrix, and the series can be truncated to provide an approximation for $\mathsf{u}$. This has several advantages. Evaluation of $L^{-1}$ scales with the square of the frequency rather than the cube, as required for $A^{-1}$ directly; subsequent terms have the same computational cost, and in any case only the first one or two terms are typically needed.

For this comparison, the FETD method was applied to a rough surface patch, embedded on an otherwise flat surface. The use of the time-domain code for this purpose has significant advantages, since it provides an entirely independent comparison and provides a physically-motivated treatment of the edge effects. The integral equation was therefore applied both to the finite rough patch itself and to the extended surface. Very good agreement was obtained for both polarizations.

In section 2 the equations, and forward-backward approximation are formulated and the FETD method described briefly. The numerical details and main results are shown in section 3.

## 2. Formulation of equations

The field in the medium can be written as a boundary integral over the normal derivative along the surface. The incident electric field is assumed to be time-harmonic, with time dependence $\exp(-\mathrm{i}_{\omega}t)$, say, and may be taken to be horizontally or vertically plane polarized, i.e. corresponding to TE or TM. We now suppress the time dependence and consider the time-reduced component, and will initially assume an incident TE field $E$. Suppose that the wave $E$ is scattered by a rough perfectly conducting one-dimensional surface $h(x)$, so that $E$ obeys the Helmholtz wave equation $(\nabla^2 + k^2)E = 0$. This is shown schematically in figure 1. Let $G$ be the free space Green's function, so that $G$ is the zero order Hankel function of the first kind,

$$G(\mathsf{r}, \mathsf{r}') = \frac{1}{4\mathrm{i}} H_0^{(1)}(k|\mathsf{r} - \mathsf{r}'|). \tag{1}$$

The governing integral equation is then obtained as

$$E_{\mathrm{inc}}(\mathsf{r}_s) = \int_{-\infty}^{\infty} G(\mathsf{r}_{\mathrm{s}}, \mathsf{r}') \frac{\partial E(\mathsf{r}')}{\partial n} \, \mathrm{d}\mathsf{r}', \tag{2}$$

where $n$ denotes the outward (i.e. downward) normal, integration is over the surface, and $\mathsf{r}_{\mathrm{s}} = (x, h(x))$ and $\mathsf{r}' = (x', h(x'))$ both lie on the surface. For convenience we write equation (2) in operator notation,

$$E_{\mathrm{inc}}(\mathsf{r}_{\mathrm{s}}) = (L + R) \frac{\partial E}{\partial n} \tag{3}$$

with the corresponding field integral

$$E_{\mathrm{s}}(x, z) = -(L + R) \frac{\partial E}{\partial n}, \tag{4}$$

where $L$ and $R$ are defined by

$$\begin{aligned} Lf(x, z) &= \int_{-\infty}^{x} G(\mathsf{r}, \mathsf{r}') f(x') \, \mathrm{d}S, \\ Rf(x, z) &= \int_{x}^{\infty} G(\mathsf{r}, \mathsf{r}') f(x') \, \mathrm{d}S \end{aligned} \tag{5}$$

and $\mathsf{r} = (x, z)$, $\mathsf{r}' = (x', h(x'))$ and $L$ includes the principal value of the integral.

Integral equation (3) has formal solution

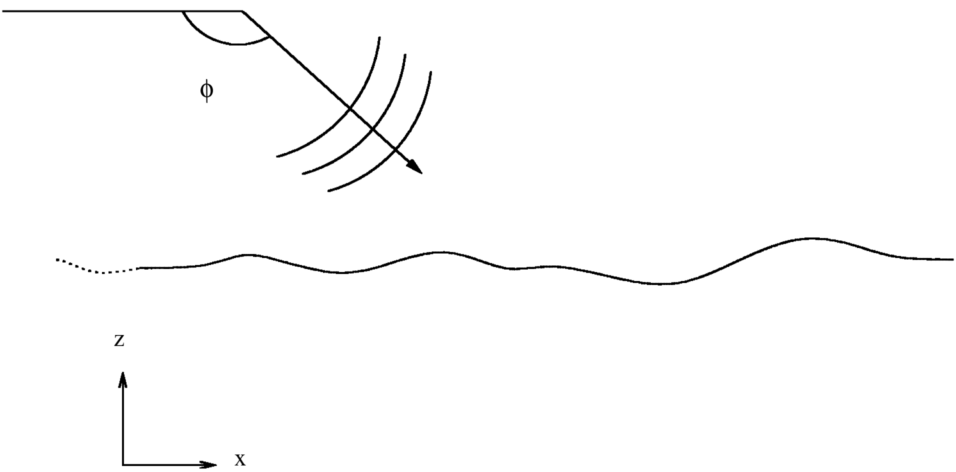


Figure 1. Schematic view of the scattering geometry.

$$\frac{\partial E}{\partial n} = (L+R)^{-1} E_{\text{inc}}, \tag{6}$$

which can be expanded in a series

$$\frac{\partial E}{\partial n} = \left[L^{-1} - L^{-1}RL^{-1} + \left(L^{-1}R\right)^2 L^{-1} - \cdots\right] E_{\text{inc}}. \tag{7}$$

Provided it converges this equation can be truncated and treated term by term. When the system is discretized, the operator $L$ yields a lower triangular matrix. Similarly $R$ becomes upper triangular (with zero on the diagonal). Inversion of the matrix $L$ can be carried out very efficiently (using Gaussian elimination and backward substitution) to give the first term of equation (7). Since subsequent terms in the series are products of $L^{-1}$ and $R$, they can also be evaluated efficiently.

Convergence of the series can be guaranteed if the effect of the operator $R$ on its argument is 'sufficiently small' compared with that of $L$ (although, as with most scattering approximations, it is very difficult to put rigorous bounds on the surface statistics which ensure convergence). Note that as surface roughness increases $R$ itself may no longer be considered small since its norm may become comparable with that of $L$. However, for predominantly right-going waves, the functions on which $R$ operates in the series (8) will all have phases which vary rapidly with $x$, so that the right half-integral represented by $R$ will give rise to functions whose amplitude is small, as required.

In the case of a TM incident field the normal derivative $H_n$ of the field at the surface vanishes, and the equation corresponding to equation (2) becomes

$$H_{\text{inc}}(\mathbf{r}_s) = H(\mathbf{r}_s) - \int_{-\infty}^{\infty} \frac{\partial G(\mathbf{r}_s, \mathbf{r}')}{\partial n} H(\mathbf{r}')\, \mathrm{d}S, \tag{8}$$

where again integration is over the surface, $n$ is the outward normal at the point $\mathbf{r}'$, and $\mathbf{r}_s = (x, h(x))$ and $\mathbf{r}' = (x', h(x'))$ both lie on the surface. (The integral in (8) must be interpreted with care, since $\partial G/\partial n$ is singular at $\mathbf{r}' = \mathbf{r}_s$. This expression corresponds to the limit of the boundary integral for a point $\mathbf{r}$ tending to the surface, $\mathbf{r} \to \mathbf{r}_s$.) Again this can be written as

$$H_{\text{inc}}(\mathbf{r}_s) = (L+R)H. \tag{9}$$

## 3. Solution and results

### 3.1. *Numerical treatment of integral equations*

The numerical solution of the equations will now be outlined. The main step is the discretization of the integral equation, and numerical solution of the resulting system. The case of TM polarization will be described here, which requires the solution of integral equation (8) or (9). (Treatment of the TE case (2) is similar, although slightly simpler due to the form of the Green's function.) The system is first discretized with respect to $x$, choosing $N$ equally-spaced points $x = x_1, \ldots, x_N$, where $x_n = n\delta$, say, and the length $\delta$ of each subinterval is small. For the moment we will ignore the question of truncation effects due to the finite surface section. The integral can then be written as a sum of subintegrals over the subintervals $[x_n, x_{n+1}]$, i.e.

$$H_{\text{inc}}(\mathbf{r}_s) = H(\mathbf{r}_s) - \sum_{n=1}^{N} \left[ \int_{x_n}^{x_{n+1}} \frac{\partial G(\mathbf{r}_s, \mathbf{r}')}{\partial n} H(\mathbf{r}')\, \mathrm{d}S \right].$$

These intervals can be chosen to be sufficiently small so that over each of them the unknown part of the integrand, $H(\mathbf{r}')$, can be treated as constant and taken outside the integral. The remaining part of the integrand is a known function which depends on the given surface profile. Writing this for each of the $N$ points $\mathbf{r}_s = (x_n, h(x_n))$, $n = 1, \ldots, N$ gives rise to a matrix equation, say

$$H_{\text{inc}} = AH. \tag{10}$$

Now define the difference $r_{ij} = |(x_i, h(x_i)) - (x_j, h(x_j))|$, and the slope variable

$$\sigma_n = [1 + h'(x_n)^2]^{1/2},$$

where the prime denotes the $x$ derivative, $h' = \mathrm{d}h/\mathrm{d}x$. The matrix entries as used in the results below are then given as follows:

$$A_{mn} = \frac{\mathrm{i}\delta}{4} \sigma_n \frac{\partial H_0^{(1)}}{\partial n}\bigg|_{kr_{mn}}, \quad \text{for} \quad m \neq n,$$

$$A_{mm} = -\left[ \frac{1}{2} - \frac{\delta}{\sigma_m^2 \pi} h''(x_m) \right]. \tag{11}$$

The term $1/2$ in the matrix entry for the case $m = n$ results from the first term on the right of equation (8) together with the appropriate limit of the integral. (Thus for a flat surface the exact solution $H = 2H_{\text{inc}}$ is recovered.) Note that the off-diagonal entries $m \neq n$ have simply been approximated by the Green's function, with a factor accounting for arc length. This arises by treating the integrand as constant over the corresponding interval and is introduced to simplify the computation. It is straightforward to improve the accuracy of this, but the approximation (11) was sufficient to give very good agreement with the FETD results.

### 3.1.1. *Left-right splitting*

System (10) can now be solved using the first few terms of the series solution (7). For example using the first two terms this becomes

$$H = (L + R)^{-1} H_{\text{inc}} \cong \left[ L^{-1} - L^{-1} R L^{-1} \right] H_{\text{inc}}. \tag{12}$$

It is straightforward to extend this to any number of terms in the series (see results below). The solution is obtained, first, for the purely right-going part, say

$$H_1 = L^{-1} H_{\text{inc}} \tag{13}$$

and a correction $H_2$ to this is then calculated, by applying the integral operator $R$ and inverting $L$ again,

$$H_2 = L^{-1}(RH_1) \tag{14}$$

to give the solution

$$H \cong H_1 - H_2.$$

When the operators $L$ and $R$ are discretized they become the triangular parts of the matrix $A$ defined in equation (11) above, i.e. $L$ is the lower-triangular part (including the diagonal) and $R$ is the upper triangular part (excluding the diagonal). The matrix $R$ is then applied in equation (14), and in equations (13) and (14) $L$ is inverted using back-substitution.

### 3.2. *Results*

The aims of this work were to examine the accuracy and convergence of the series approximation, for both TE and TM waves, by comparison with independent results, and to assess the effect of truncation of the computational domain.

The comparison allows us to focus on the surface current, which is the central source of computational difficulty. The reradiated fields are obtained from this by a straightforward integration, which is the same for both methods; this quantity is therefore not examined here.

Two sample rough corrugated surfaces were generated for this comparison, as shown in figures 2 (*a*) and (*b*). These were taken from ensembles having Gaussian and 4th order power-law autocorrelation functions $\rho(\xi)$, given respectively by

$$\rho(\xi) = \sigma^2 \exp\left(-\xi^2/L^2\right)$$

and

$$\rho(\xi) = \sigma^2(1 + |\xi|) \exp\left(-|\xi|/L\right),$$

where the scaling factor $L$ determines the autocorrelation length scale. The first is relatively smooth and the second fairly jagged at a small scale. These produced significant differences in the scattering solution. For this comparison the surface

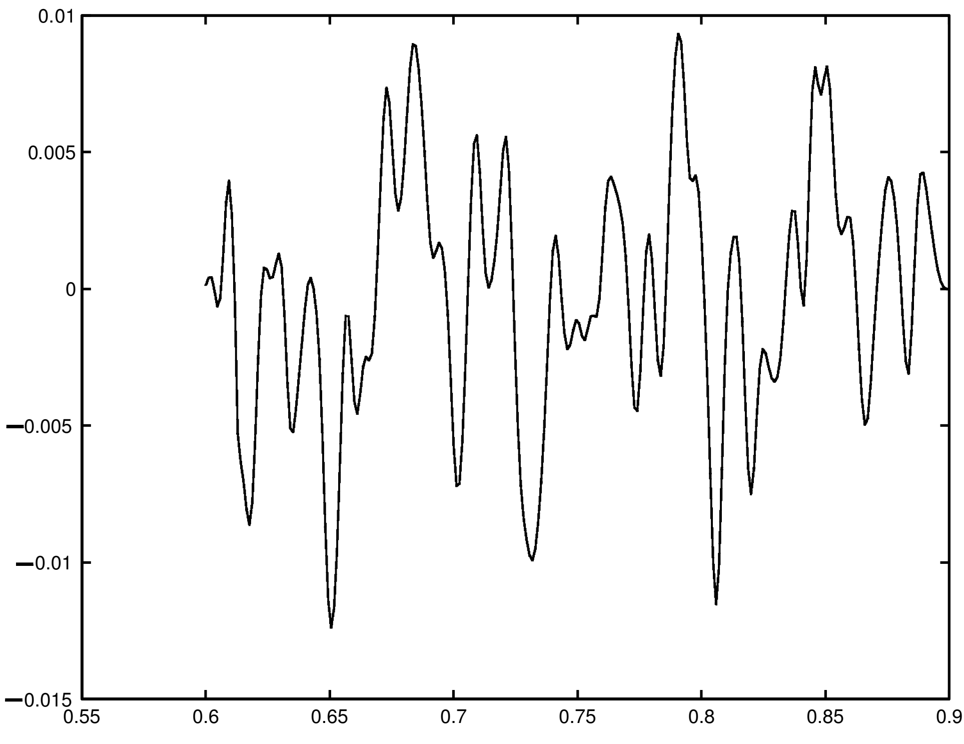


Figure 2 (*a*). Rough surface with Gaussian autocorrelation function used in these results.

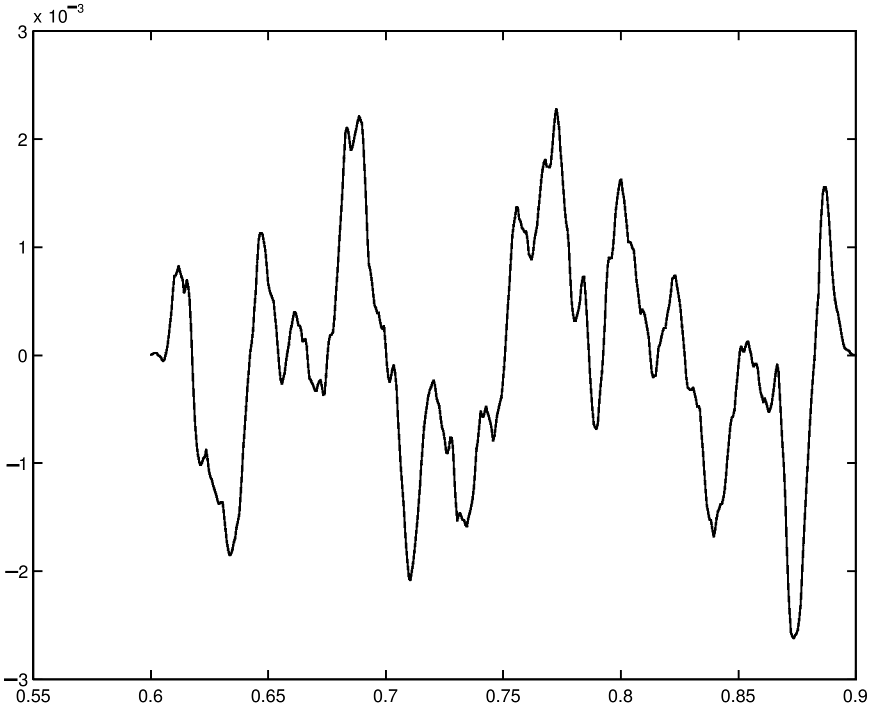


Figure 2 (*b*). Rough surface with 4th order power-law autocorrelation function in these results.

variation was tapered to zero at the ends, by applying a tapering function over a distance less than $L$. The rough surfaces themselves were approximately $10\lambda$ in length, and scale size was of the order of a wavelength, $L = \lambda$. For some of the calculations the rough surface was embedded on a larger, otherwise flat, surface, and the simulations were run using up to a maximum of 8192 points. The frequency of the incident field was 10 GHz, so that $\lambda = 0.03$ m and the rough surface length was around 0.3 m. Typical peak-to-trough heights in the case of the TM simulations were 4 mm, i.e. around $\lambda/7$, and 20 mm in the TE case. (The larger figure was taken for TE in order to ensure easily measurable field effects.)

In both cases the solutions represent the vector surface currents $\mathbf{J}(x)$. (The problem reduces to a scalar one since $\mathbf{J}$ lies in the plane of the surface, say $\mathbf{J} = J\mathbf{t}$, where for TM $\mathbf{t}$ is tangential to the surface in the $(x, z)$ plane and $\mathbf{t}$ is parallel to the $y$ direction for TE.)

Comparative numerical results have been generated using 2D Finite Element Time Domain software. This is a node-based Taylor-Galerkin multi-material implementation on an unstructured triangular mesh. Either first order Higdon or dissipative layer boundary conditions may be used within a scattered field formulation. In addition, CW or pulsed excitation may be applied. Figure 3 shows the 2D computational domain used in this study, comprising the rough, perfectly conducting, surface embedded in an otherwise smooth, flat, perfectly conducting, surface. The shape and size of the computational domain and the boundary conditions used avoids any possible problems that might be associated

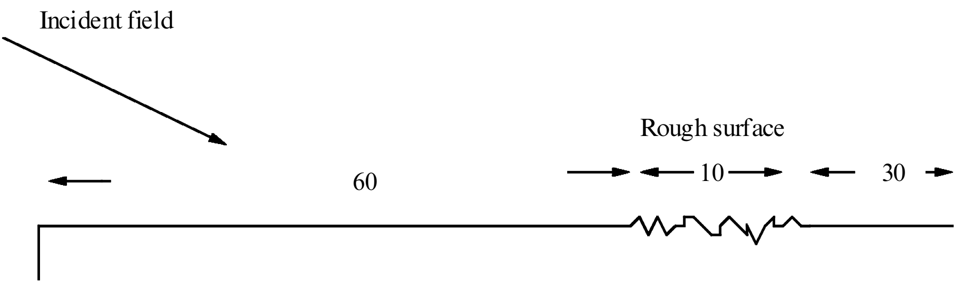


Figure 3. Schematic view of 2-dimensional computational domain for the finite element time domain calculation, showing a rough surface embedded in an otherwise flat surface. Values refer to sizes in terms of wavelength.

with energy reflected from the boundaries of the computational domain. The length of the flat sections was varied according to the polarization of the incident field. For TE, the left-hand section was $20\lambda$ and the right was $10\lambda$; in the case of TM incidence the left was taken to be $60\lambda$ and the right $30\lambda$. In all cases the section of rough surface was sampled at 512 points, giving a typical mesh element length of around $0.02\lambda$ in the region containing the rough surface.

3.2.1. *TM polarization*

3.2.1.1 *Truncated surface.* The solution above was first obtained on the rough surface section alone, for a field incident at a grazing angle of $10^\circ$, for the smoother Gaussian surface. Figure 4 shows the comparison between this and the FETD result, for the amplitude $|\mathbf{J}|$. For the series solution, the first two terms were taken, i.e. 'right-going' plus single left-going interaction. The current density would be $2\,\mathrm{A\,m^{-1}}$ on an infinite flat surface. Detailed agreement is found to be remarkably good, particularly in view of the significant 'reflected' and transmitted waves present in the FETD results at each end of the rough surface patch.

The importance of including some left-going interaction is clear from figure 5, which shows the poorer agreement when only the first term in the series is used.

Similar results were obtained when the methods were applied to the more jagged 'power-law' surface. Comparison between current amplitudes from FETD and the first two terms of the series are given in figure 6. Very close agreement is again seen.

It is noticeable that, even when surface currents are evaluated on the truncated rough surface patch, close agreement is obtained with FETD results on that segment. This suggests that the formulation is robust, and is a consequence of the inclusion of the delta-function term in the solution, represented by the 1/2 in equation (11).

3.2.1.2 *Extended surface.* The effects of truncation on the series solution were also examined by embedding the surface on a longer, otherwise flat, surface. This was done for the Gaussian surface above. Figures 7 (*a*) and (*b*) show the resulting surface current for (*a*) the first term only and (*b*) the first two terms. The reflection to the left seen in (*b*) is almost indistinguishable from that of the FETD results; this reflection cannot appear in (*a*) since the first term does not allow for any left-travelling energy.

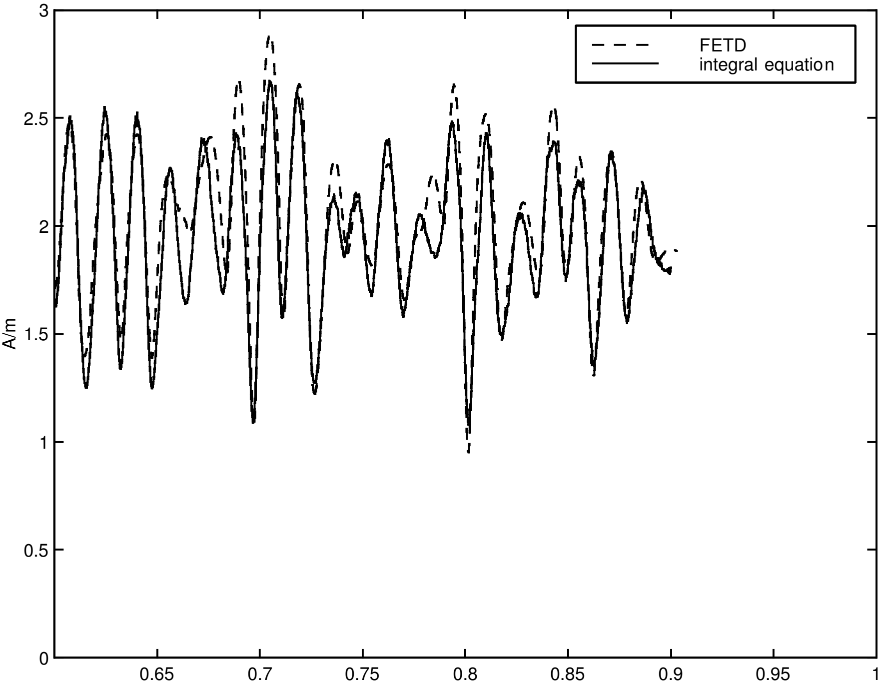


Figure 4. Comparison between the current amplitude for the TM field incident at a grazing angle of 10° on a Gaussian surface, for the first two terms of the series solution.

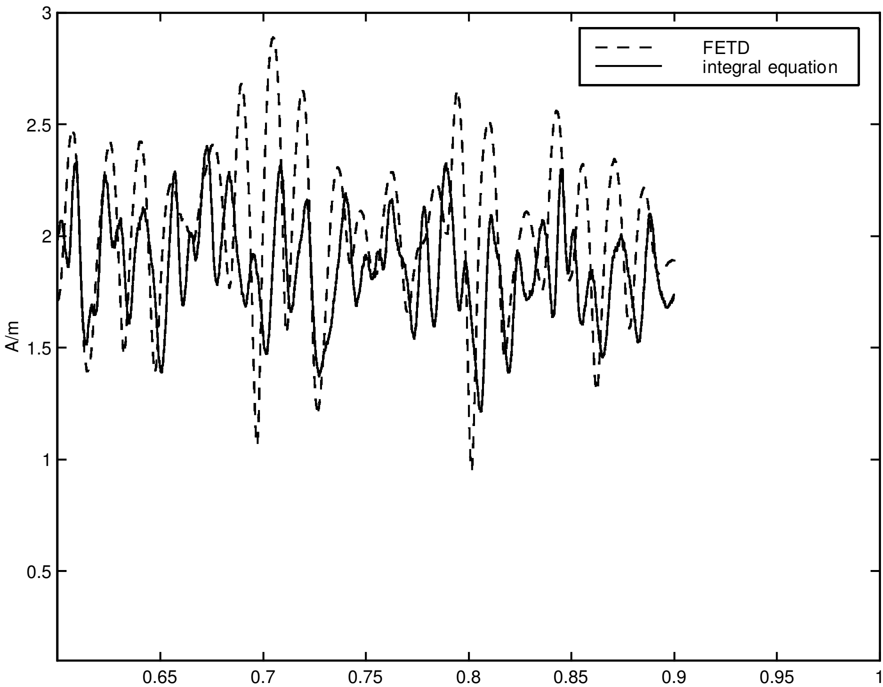


Figure 5. Comparison with the case of figure 4, using only the first term series solution.

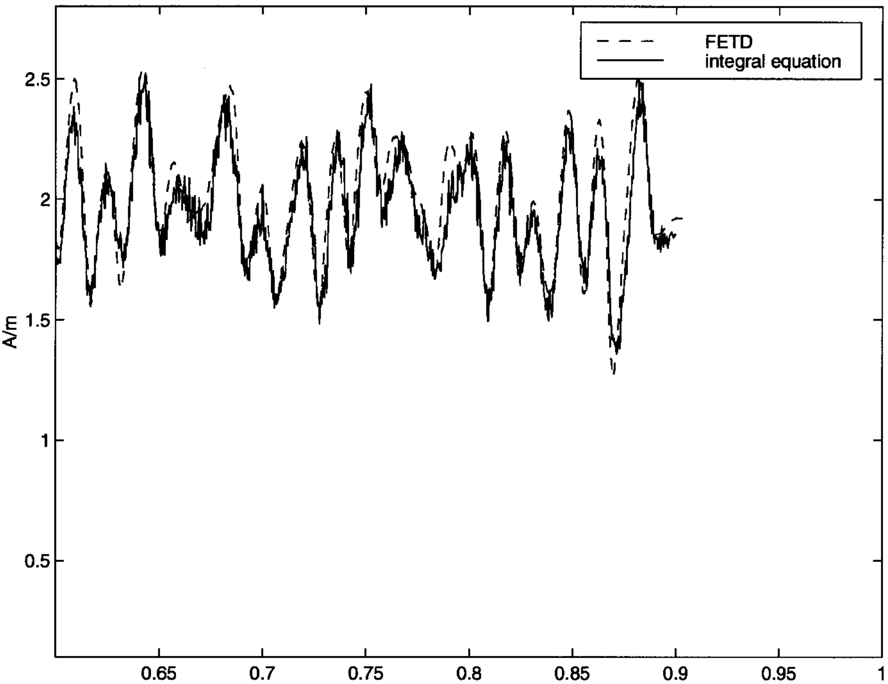


Figure 6. Comparison between the current amplitude for the grazing angle 10° on the power-law surface, for the first two terms of the series solution.

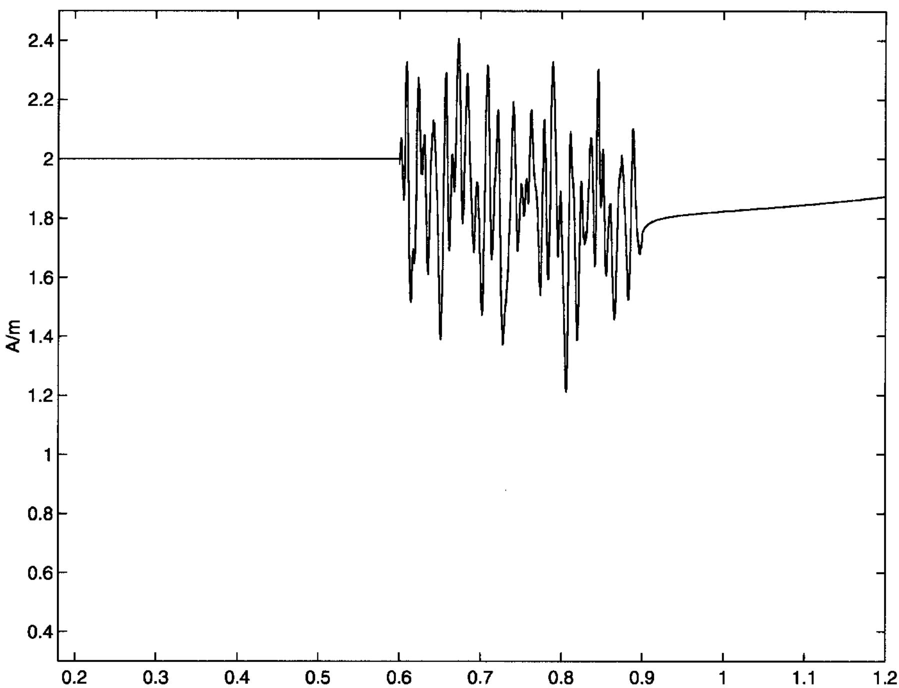


Figure 7 (*a*). Comparison between series and FETD solutions, when a Gaussian surface is embedded in an otherwise flat surface in the series solution, showing first term only.

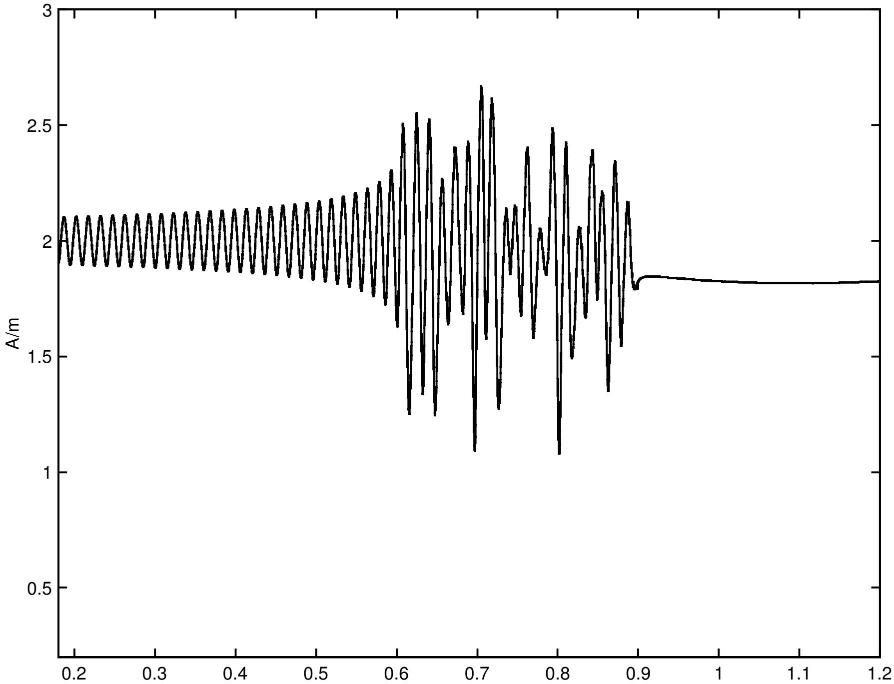


Figure 7 (*b*). Comparison between series and FETD solutions, when a Gaussian surface is embedded in an otherwise flat surface in the series solution, showing the first two terms.

3.2.2. *TE polarization*

Scattering of the TE field is much less significant for the same surface, and the height of the Gaussian surface of the previous calculations was therefore increased by a factor of 5 to produce useful data, as discussed above. The current density here would be $2\sin 10^{\circ}\,\mathrm{A\,m^{-1}}$, or about $0.35\,\mathrm{A\,m^{-1}}$ on an infinite flat surface. As shown in figure 8 good agreement is obtained. This calculation was carried out for the extended surface described above. It is worth noting that the current takes a distinctly different form compared with TM polarization, with very low nulls and high narrow peaks.

Although TE scattering for a given surface is weaker than for a TM polarized field, the matrix $A$ is less diagonally dominant, and the solution is consequently far more sensitive to surface truncation. The interaction of an incident plane wave with the edge of the surface in this case produces high peaks in the surface current at the edges, with a tail which may persist for several wavelengths. This can be circumvented by use of a tapered plane wave [19] (i.e. by tapering the incident field so that it is nearly zero at the edge of the numerical domain). However, this can also influence the resulting surface current over several wavelengths, well beyond the width over which the incident field is tapered.

In these results the time required for solution of surface currents by the splitting method was typically a few seconds on a Dec Alpha workstation. This scales with $O(N^2)$ (per iteration), where $N$ is the number of points in the surface discretization. Equivalently, it increases with $\lambda^{-2}$, where $\lambda$ is the wavelength. This compares with an order $O(N^3)$ dependence for a method-of-moments calculation.

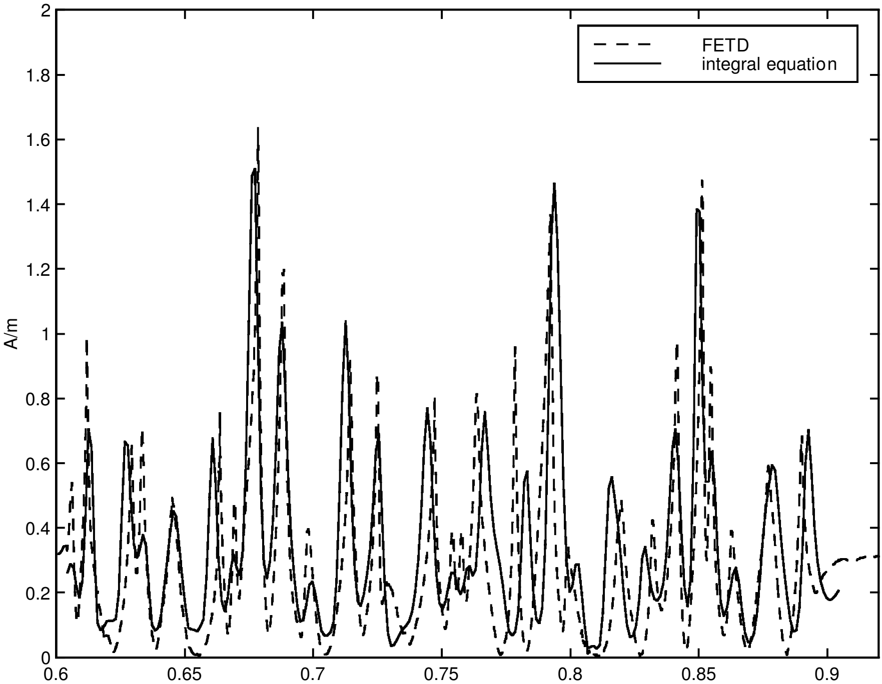


Figure 8. Comparison for the case of an incident TE field, on a Gaussian surface, showing two terms of the series solution.

The FETD computation was considerably slower, requiring several minutes on a workstation, but this comparison is misleading as the FETD was chosen to provide an accurate independent validation and was not optimized for computation time.

## 4. Conclusions

The method of left-right splitting has been developed and applied to characterized rough surfaces, and the results compared with finite element time domain calculations. This has been carried out for TE and TM polarized fields (i.e. Dirichlet and Neumann boundary conditions respectively), and for perfectly conducting surfaces. This method has the advantage of computational efficiency, while retaining the ability to describe high-order multiple scattering.

In most cases remarkably good agreement was obtained with FETD calculations using one or two terms of the series. In order to obtain surface currents by the FETD method the rough surface patch was embedded on a longer, otherwise flat, surface. The series solutions were obtained both on the truncated rough surface patch itself and on the extended surface. For the more important TM polarization good agreement was found on the rough surface patch, even when the truncated surface is used, and the reflected and propagating fields to the left and right respectively are accurately reproduced when the extended surface is used. This is attributable to the form of the integral equation, for which the first term reduces to the exact solution in the limit of a flat finite surface. In the TE case, however, singularities arise at the edge of the computational domain unless the field is tapered to zero there. The resulting distortion of the solution extends over two or three wavelengths, so that the extended surface is required in order to adequately model the surface current.

The idealized assumption of perfect conductivity is an accurate model for many physical problems, and provides a useful basis for validation, excluding scattering mechanisms due to dielectric interfaces. The splitting method described here extends naturally to such interface problems; however, as surface waves are then supported, much greater care is needed in dealing with edge truncation.

## Acknowledgments

This work was carried out under a project on electromagnetic scattering funded by BAE Systems, Sowerby Research Centre.

## References

[1] Ogilvy, J. A., 1991, *The Theory of Wave Scattering from Random Rough Surfaces* (Bristol: IOP Publishing).
[2] Voronovitch, A. G., 1994, *Wave Scattering from Rough Surfaces* (Berlin: Springer).
[3] Nieto-Vesperinas, M., and Sotocrespo, J. M., 1987, *Optics Lett.,* **12,** 979.
[4] Maradudin, A. A., Mendez, E. R., and Michel, T., 1989, *Optics Lett.,* **14,** 151.
[5] Maystre, D., Mendez, O. M., and Roger, A., 1983, *Opt. Acta,* **30,** 1707.
[6] Saillard, M., and Maystre, D., 1990, *J. opt. Soc. Am.* A, **7,** 982.
[7] Brown, G. S. (ed.), 1998, *IEEE Trans. Ant. Prop.,* **46,** special issue on low-grazing-angle backscatter from rough surfaces.
[8] Thorsos, E., 1987, *J. acoust. Soc. Am.,* **82**(Suppl. 1), S103.
[9] Spivack, M., 1995, *J. acoust. Soc. Am.,* **97,** 745.
[10] Kapp, D. A., and Brown, G. S., 1996, *IEEE Trans. Ant. Prop.,* **44,** 711.
[11] Spivack, M., 1994, *J. acoust. Soc. Am.,* **95,** 3019.
[12] Macaskill, C., and Kachoyan, B. J., 1993, *Appl. Optics,* **32,** 2839.
[13] Thorsos, E. I., and Jackson, D. R., 1989, *J. acoust. Soc. Am.,* **86,** 261.
[14] Holford, R. L., 1981, *J. acoust. Soc. Am.,* **70,** 1116.
[15] DeSanto, J. A., 1981, *Radio Sci.,* **16,** 1315.
[16] Meecham, W. C., 1956, *J. Rat. Mech. Anal,* **5,** 323.
[17] Voronovich, A. G., 1985, *Sov. Phys. JETP,* **62,** 65 [translated from *Zh. Eksp. Teor. Fiz.*].
[18] Voronovich, A. G., 1996, *Waves in Random Media,* **6,** 151.
[19] Thorsos, E. I., 1988, *J. acoust. Soc. Am.,* **83,** 78.